Biogeosciences, 8, 137–146, 2011
www.biogeosciences.net/8/137/2011/
doi:10.5194/bg-8-137-2011

Biogeosciences

Oxygenation variability in Mejillones Bay, off northern Chile, during the last two centuries

J. A. Díaz-Ochoa[1,*], S. Pantoja[1], G. J. De Lange[2], C. B. Lange[1], G. E. Sánchez[1], V. R. Acuña[1], P. Muñoz[3], and G. Vargas[4]

[1]Departamento de Oceanografía and Centro de Investigación Oceanográfica en el Pacífico Sur Oriental (FONDAP-COPAS), Universidad de Concepción, Casilla 160-C, Concepción, Chile
[2]Geochemistry Department, Faculty of Geosciences, Utrecht University, Budapestlaan 4, 3584 CD, Utrecht, The Netherlands
[3]Departamento de Biología Marina, Universidad Católica del Norte, Larrondo 1281, Coquimbo, Chile
[4]Departamento de Geología, Universidad de Chile, Casilla 13518 Correo 21, Plaza Ercilla 803, Santiago, Chile
[*]now at: Departamento de Ciencias y Recursos Naturales, Universidad de Magallanes, Avenida Bulnes 01855, Casilla 113-D, Punta Arenas, Chile

Received: 4 June 2010 – Published in Biogeosciences Discuss.: 1 July 2010
Revised: 14 December 2010 – Accepted: 19 December 2010 – Published: 20 January 2011

Abstract. The Peru Chile Current ecosystem is characterized by high biological productivity and important fisheries. Although this system is likely to be severely affected by climate change, its response to current global warming is still uncertain. In this paper, we analyze 10–166 year-old sediments in two cores collected from Mejillones Bay, an anoxic sedimentary setting favorable for the preservation of proxies. Based on a 166-year chronology, we used proxies of bottom-water oxygenation (Mo, V, S, and the (lycopane+n-C_{35})/n-C_{31} ratio) and surface water productivity (biogenic opal, counts of diatom valves, biogenic Ba, organic carbon, and chlorins) to reconstruct environmental variations in Mejillones Bay. During the last two centuries, a shift took place in the coastal marine ecosystem of Bahia Mejillones at decadal scales. This shift was characterized by intense ENSO-like activity, large-scale fluctuations in biological export productivity and bottom water oxygenation, and increased eolian activity (inferred from Ti/Al and Zr/Al). This short-term variability was accompanied by a gradual increase of sulfidic conditions that has intensified since the early 1960s.

Correspondence to: J. A. Díaz-Ochoa
(jadiaz@udec.cl)

1 Introduction

Eastern boundary upwelling systems such as Peru-Chile, California, Canary, and Benguela are amongst the richest areas for world fisheries, concentrating ∼10–20% of the world catch in ∼0.1% of the global ocean (Chavez et al., 2008; Fréon et al., 2009). With the exception of the Canary Current, these eastern boundary upwelling systems are characterized by the formation of an intense mid-water depth oxygen minimum zone (OMZ) fueled by high levels of organic matter respiration, sluggish circulation, and/or the advection of low oxygen waters (Helly and Levin, 2004). The study of such oxygen-deficient layers is of particular interest because of their contribution to oceanic-atmospheric gas exchanges, including CO_2, at both regional and global scales (Fréon et al., 2009). Several studies recently pointed out that anoxia increased in the world ocean as the climate warmed over the last century (Chan et al., 2008; Diaz and Rosenberg, 2008; Monteiro et al., 2008; Stramma et al., 2008, Keeling et al., 2010 and references therein). This work focuses on OMZ variability within the Peru-Chile Current System, specifically in a shallow bay of northern Chile (Mejillones Bay) and its relation with biological productivity during the last two centuries.

The OMZ off Peru and Chile is relatively shallow (<100–∼600 m deep, dissolved oxygen <22 micromol L^{-1}) and strongly affected by the occurrence of El Niño (EN) events at interannual timescales. During EN events, warm water masses from the western equatorial Pacific Ocean intercept

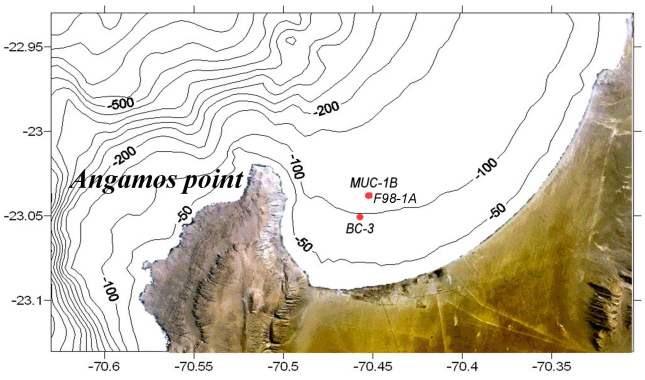

Fig. 1. Study area, Mejillones Bay, and sampling locations of cores MUC-1B, BC-3, and F98-1A.

coastal upwelling zones, oxygenating the shelf and upper slope (Blanco et al., 2002; Arntz et al., 2006; Fuenzalida et al., 2009, and references therein). At longer time scales, enhanced organic carbon burial and stronger reducing conditions in the sediments have been inferred using sediments from AD 1820 to 1878 collected in northern Chile and southern Peru (Vargas et al., 2007). This shift has been associated with centennial-scale intensification of southerly winds, enhanced upwelling of nutrients to the euphotic zone, and increased primary production as well as with less environmental oxygenation (Vargas et al., 2004, 2007; Siffedine et al., 2008).

In this paper, we use information provided by redox-sensitive elements (Mo, V, and S) and the (lycopane+n-C_{35})/n-C_{31} ratio preserved in the sediments as bottom-water oxygenation proxies. The paleoxygenation signal is examined in a multi-proxy framework considering biological productivity and historical El Niño Southern Oscillation (ENSO) events. Thus, we are able to reconstruct the upper sediment and water column redox conditions during the last two centuries, to assess underlying mechanisms responsible for oxygenation variations at decadal scales, and to provide insight on the response of the Peru-Chile upwelling ecosystem to recent climate change.

2 Study area

Mejillones Bay (∼23°S–∼70°25′ W, off the Atacama Desert) is a relatively shallow water body (depth <125 m) in the Peru-Chile Current System (Fig. 1), characterized by high biological productivity (1070 g C m^{-2} yr^{-1}; Marin et al., 1993), restricted water circulation, and low turbulence. Here, very low dissolved oxygen concentrations ([O_2] <44 micromol L^{-1}) are typical at water depths below 50 m, and near-anoxic conditions ([O_2] <4 micromol L^{-1}) develop in the bottom water (Escribano, 1998; Marin et al., 2003; Valdés et al., 2003; Vargas et al., 2004).

Off northern Chile, oceanic circulation is dominated by the Peru-Chile Current (PCC), which transports SubAntarctic Water (SAW) from higher to lower latitudes. The PCC is split into an oceanic and a coastal branch by the Subtropical Surface Water of the Peru Chile Countercurrent (PCCC) (Strub et al., 1998). A Poleward Undercurrent moving below the PCC and the PCCC transports oxygen-depleted Equatorial Subsurface Water and defines the OMZ off northern Chile between 50 and 300 m (Morales et al., 1999). Below 500 m depth, Antarctic Intermediate Water flows to the equator. Therefore, oxygen-depleted conditions in Mejillones are partly due to the location of this bay within the eastern South Pacific OMZ and partly to the high primary productivity levels associated with the quasi-permanent upwelling off Angamos Point and high organic matter respiration rates (Morales et al., 1999; Marin et al., 2001). Sea surface temperatures within Mejillones Bay may be higher than in the surrounding sea, even during active upwelling, due to the upwelling shadow (Marín et al., 2001). This is a mesoscale feature occurring in spring-summer that helps isolate this area through the formation of a thermal front (Marín et al., 2001, 2003; Vargas et al., 2004).

Several studies conducted on the 1997–1998 El Niño phenomenon suggested that these general circulation and temperature patterns may be altered by the presence of Kelvin poleward waves, which increase sea surface temperature and deepen both the thermocline and the oxycline (e.g. González et al., 1998; Iriarte et al., 2000; Fuenzalida et al., 2009). Presently, sediments in Mejillones Bay are deposited under very low oxygen conditions, allowing good preservation of organic matter and biogenic proxies such as diatom valves, tests of foraminifers, and fish scales within the laminated sediments (e.g. Ortlieb et al., 2000; Valdés et al., 2004; Vargas et al., 2004; Vargas et al., 2007; Díaz-Ochoa et al., 2008; Caniupán et al., 2009). High rates of primary productivity promote high export rates of agglomerated (brown and black) organic matter and high rates of sulfate-reduction and redox-sensitive trace metals are removed from bottom water to surface sediments in the form of metallic sulfurs (Valdés et al., 2004), as observed in other hypoxic environments (e.g. Santa Barbara Basin; Zheng et al., 2000). On the other hand, periods of lower primary productivity, organic matter deposition, and sulfate reduction rates are recorded as dispersed and yellowish organic matter (Valdés et al., 2004).

Mejillones Bay provides a privileged setting for paleoceanographic reconstructions and its sedimentary record appears to reflect conditions for the adjacent coastal ecosystem (Vargas et al., 2007).

3 Material and methods

We analyzed two sediment cores collected during the ZOMEI cruise aboard the AGOR Vidal Gormáz of the Chilean Navy, between 25 September and 1 October 2005 in Mejillones Bay.

The first core was collected with a box corer at 23°03.3′ S, 70°27.4′ W (BC-3; Fig. 1). This core was subsampled on board using four acrylic plates (BC-3A to BC-3D; dimensions 50 cm×10 cm) to obtain vertical sediment slabs that were stored at 2 °C for further analysis in the laboratory. One of the acrylic plates (BC-3C) was subsampled with a resolution of 0.5 cm for dating based on ^{210}Pb activities (Caniupán et al., 2009). Another plate (BC-3D) was used for measuring the contents of biogenic opal (SiO_2), organic carbon (C_{org}), and chlorins, and for analyzing physical properties (i.e. water content, dry bulk density, and magnetic susceptibility; this and the other proxy data for BC-3 are available from Caniupán et al., 2009). Plate BC-3D was dated by lateral correlation with plate BC-3C using magnetic susceptibility profiles. Magnetic susceptibility measurements were made with a Spinning Specimen Magnetic Susceptibility Anisotropy Meter, model KLY-3S developed by AGICO Inc. Three measurements were made for each sample, and the values were normalized by sample volume and averaged (mean measurement error $\pm 0.03\,cm^{-3}\times10^{6}$ SI units; Caniupán et al., 2009).

Organic carbon in core BC-3 was measured from ∼10 mg of wet sediment samples dried at 50°C within a 0.6 N HCl atmosphere for 5 h to remove inorganic carbon and determined with an elemental analyzer at University of California, Davis, USA. Although the information of BC-3 was acquired with laminae resolution (thickness varying between 2 and 10 mm), in this paper, we present the results averaged in 0.5-cm intervals to allow comparisons with the second core, which was sampled at the same resolution (see below).

The second core was collected with a multicorer at 23°2.6′ S, 70°27.1′ W (MUC-1B; Fig. 1). Core MUC-1B was sectioned onboard every 0.5 cm and samples were stored in plastic bags at 4 °C. Sections of this core were freeze-dried, powdered with an agate mortar, and subjected to a mixture of strong acids (72% $HClO_4$, 4.5% HNO_3, and 48% HF) for determining elemental composition (Al, Ba, Fe, Mo, Na, S, Ti, V, Zr) with an inductively coupled plasma optical emission spectrometer (ICP-OES) according to Schenau and De Lange (2000). Despite the laminated nature of the sediments that accumulate in Mejillones Bay, the resolution of the samples from MUC-1B was lower (0.5 cm) and this analysis is not intended to be carried out to lamina resolution.

The productivity proxies used for core MUC-1B were biogenic opal measured following Mortlock and Froelich (1989), counts of diatom valves (Sánchez, 2009), and the content of biogenic Ba (bioBa) extracted from the core with 2M NH_4Cl (pH = 7) at several intervals following the method of Rutten and De Lange (2002). We also estimated biogenic Ba (Ba_{bio}) using the normative method assuming that Ba_{bio} is the difference between the total Ba (Ba_{tot}) content and the detrital Ba fraction estimated by: $Ba_{bio} = Ba_{tot} - (Al \times (Ba/Al)_{det})$ (Reitz et al., 2004). Estimates of detrital Ba/Al ($(Ba/Al)_{det}$) between 0.001 and 0.003 were obtained from the samples using the formula: $(Ba/Al)_{det} = (Ba_{total} - Ba(NH_4Cl$ extraction solution))/(Al – Al (NH_4Cl extraction solution)). These estimates of detrital Ba/Al (mean resolution of ∼1 cm) were averaged and their standard deviations were computed.

All the elements measured by ICP-OES were normalized with Al to correct for variable detrital input. Percent deviations from the mean were estimated for Ti/Al and Zr/Al and their summation was used as a proxy for terrigenous material input. Mo/Al and V/Al were interpreted as paleoredox proxies, whereas S/Al was corrected for seawater salt content and used as a proxy of sulfate reduction intensity (Nameroff et al., 2004; Böning et al., 2005).

In addition, we studied the depth variation of the ratio (lycopane+n-C_{35})/n-C_{31} as an organic paleoredox proxy since preservation of lycopane is enhanced under anoxic conditions (e.g. Sinninghe Damsté et al., 2003). Lycopane was extracted from ∼0.6 g sediment samples of MUC-1B and analyzed using an Agilent Technologies 6890 instrument equipped with an Agilent Technologies 5973 mass spectrometer. The chromatograph was equipped with a fused silica capillary column (30 m length, i.d. = 0.25 mm HP5-MS, film thickness = 0.25 µm) and an automated injection system. Helium was used as the carrier gas (101.9 kPa pressure) with a flow of 24.4 mL/min. The oven was programmed from 80 °C to 130 °C at a rate of 20 °C/min, and then to 310 °C (32.5 min) at a rate of 4 °C/min. The mass spectrometer was programmed to 70 eV and compounds were identified based on the relative retention time and by comparison with mass spectra reported in literature (Kimble et al., 1974; Volkman, 2005).

3.1 Chronology of sediments

A chronology for MUC-1B was established by measuring ^{210}Pb activity with a Canberra Quad Alpha 7404 Spectrometer at the radioisotope laboratory of the Universidad de Concepción. Ages were computed using the constant rate of supply model (CRS; Appleby and Oldfield, 1978; Binford, 1990). At core depths for which CRS could not be used, we employed stratigraphic correlations with two other dated cores collected at the same location (i.e. $CaCO_3$ content of core F98-1A collected in 1998, Vargas et al., 2007) and at a nearby location (i.e. several stratigraphic features observed in core BC-3 by Caniupán et al., 2009, see below) to extrapolate ages downcore by simple linear regression. MUC-1B was correlated with core BC-3D using the presence of a "spongy" layer (see description in section 4.1) and a disturbed layer caused by dredging of the Mejillones harbor (Grillet et al., 2001; Caniupán et al., 2009). It should be noted that this dredging at the end of 2002 resuspended the sediment in the upper ∼5 cm of BC-3 and was associated with higher magnetic susceptibility values and high Fe contents by Caniupán et al. (2009).

To analyze the connections between the several proxies measured in the sedimentary record for this study and climatic and oceanographic variability in the study area, this

work includes a list of ENSO events per Quinn et al. (1987), Quinn (1993), Garcia-Herrera et al. (2008), and Gergis and Fowler (2009) for events prior to AD 1950 and Trenberth (1997) for events after AD 1950. The documentary sources of historical ENSO events (El Niño and La Niña) are complemented by an analysis of a time-series of mean sea surface temperature anomalies in the central equatorial Pacific (6° N–6° S, 180–90° W). Known as the cold tongue index (CTI), this is an indicator of the ENSO phenomena (Joint Institute for the Study of the Atmosphere and Ocean; http://jisao.washington.edu/data/cti/). Moreover, we interpret the sedimentary proxy records at multidecadal scales, taking into account a reconstructed Pacific Decadal Oscillation (PDO) series derived from tree-ring data for sensitive regions of coastal Alaska, the Pacific Northwest, and subtropical North America (D'Arrigo et al., 2001). Instrumental records of the PDO since AD 1900 are also included in the analysis (Mantua et al., 1997).

Table 1. List of strong, very strong, and extended El Niño and La Niña events included in core MUC-1B chronology. The El Niño historical events before AD 1950 are taken from Quinn et al. (1987), Quinn (1992), Garcia-Herrera et al. (2008), and Gergis and Fowler (2009). La Niña events correspond to those reported by Gergis and Fowler (2009). After AD 1950, ENSO events correspond to events longer than or equal to 12 months (Trenberth, 1997).

El Niño		La Niña		
1844–1845	1932	1847	1892–1894	1988–1989
1861–1864	1940–1941	1860–1861	1916–1918	1998–1999
1869–1871	1957–1958	1863	1922	–
1877–1878	1972–1974	1867–1868	1946	–
1883–1884	1982–1983	1870–1871	1950–1951	–
1888-1891	1986-1988	1873-1875	1954-1956	–
1899–1900	1992	1878–1880	1970–1972	–
1908–1910	1997–1998	1887	1973–1974	–
1925–1926	–	1890	1974–1976	–

4 Results

4.1 Sediment characteristics

Both BC-3 and MUC-1B were mostly olive green-gray in color (Munsell chart scale 7.5Y 3/2), with a succession of dark and light layers. A spongy layer (green rectangles in Figs. 2a, b, d) was found in both cores and was considerably bright (Munsell scale 7.5Y 4/4; e.g. the band between AD 1861 and 1870 of core BC-3 in Fig. 2e), with high water content (MUC-1B: >90% w/w) and low density (MUC-1B: $<0.1\,g\,cm^{-3}$). The sediments in cores MUC-1B and BC-3 were also rich in biogenic opal (MUC-1B: ∼17->50% – SiO_2 vs. BC-3: ∼19–55 %-SiO_2; Fig. 3a) and diatom valves (MUC-1B: $<1\times10^8$ and $>10\times10^8$ valves g^{-1} ; Fig. 3b), Ba_{bio} (MUC-1B: 90-355 ppm; Fig. 3c), chlorins (MUC-1B: 197–735 $mmol\,g^{-1}$; Fig. 3d), C_{org} (BC-3: 1–9%; Fig. 3e), and fish debris (MUC-1B: Díaz-Ochoa et al., 2008). In general, we observed a negative relationship between dry bulk density values and biogenic opal and diatom valve counts in core MUC-1B (data not shown), and lower density/higher biogenic opal values tended to be found within lighter layers (Figs. 2e; 3a–b).

4.2 Chronology

Figure 2 shows a comparison of several proxy data in cores MUC-1B, F981-A, and BC-3. In core MUC-1B, high and relatively uniform values of ^{210}Pb are apparent within the uppermost 4.5 cm, similar to the pattern in the top 5 cm of core BC-3. The highest values of Fe/Al are attained in the top of core MUC-1B, coinciding with high values of magnetic susceptibility in the upper layers of core BC-3 (Figs. 2a, d). In addition, several %$CaCO_3$ peaks in cores MUC-1B and F98-1A were correlated (Figs. 2b, c) and an alignment of the spongy layers of cores MUC-1B and BC-3 was possible (green areas in Figs. 2a, b, d). A final integrated age model for core MUC-1B, the result of the combination of the CRS model fitted to ^{210}Pb excess in the upper 10 cm (at core depths >10 cm, several anomalous ^{210}Pb values violated the steady state assumption; Fig. 2f) and stratigraphic correlations with cores F98-1A and BC-3, permitted a linear extrapolation of ages deeper downcore (Fig. 2g). A chronology of strong to very strong/extended historical ENSO events is also provided (Table 1).

4.3 Paleoproductivity proxies

The biogenic opal time-series in BC-3 exhibits a pronounced decreasing trend from the late 1780s (>50% SiO_2) to ∼1840 through the early 1860s (<30% SiO_2). The last part of this long-term trend is also captured by core MUC-1B in the early 1840s (Fig. 3a). We note two major features of the biogenic opal series in cores MUC-1B and BC-3: on one hand, this record becomes more variable since the early ∼1860s and on the other hand, the decreasing trend observed during the early 19th century inverts, with greater concentrations of biogenic opal found from the second half of the 19th century and throughout the 20th century, peaking in the early 1950s. From the early 1960s, a clear decreasing trend in biogenic opal is observed, especially for MUC-1B (Fig. 3a). Unlike the long-term trends at shorter time scales, the biogenic opal record in MUC-1B and BC-3D seems mostly out of phase with the exception of two relatively brief intervals during the 1860s (the spongy layer) and the 1950s (Fig. 3a). It is also interesting to note that biogenic opal in the spongy layer (∼1860s) was extremely variable and that diatom valves declined abruptly (from $\sim10\times10^8\,g^{-1}$ to $\sim<2\times10^8\,g^{-1}$) in this layer from 1863 until the end of the decade, whereas valves of oceanic/warm-water species increased by a factor ∼>2 (Table 2).

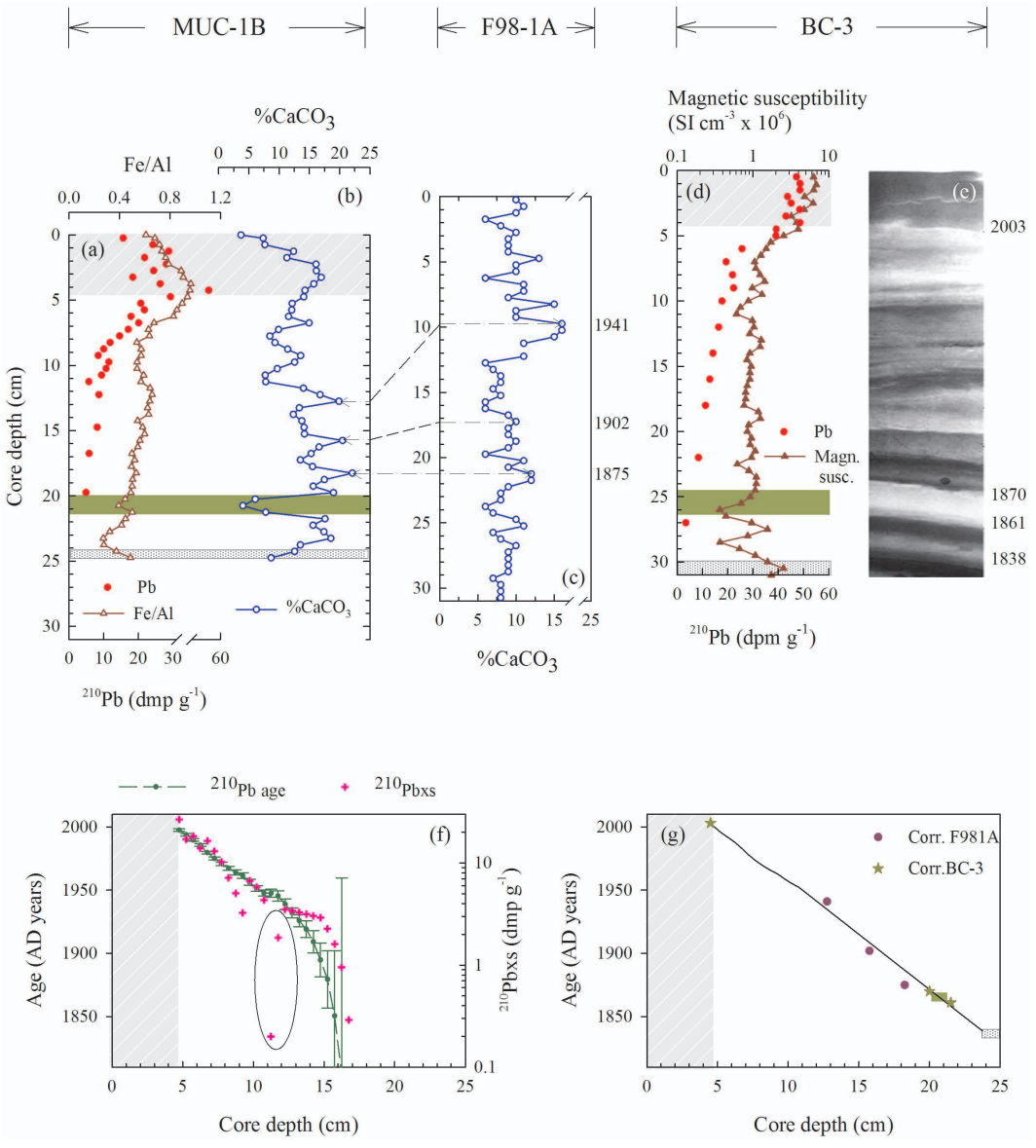

Fig. 2. Fe/Al and ^{210}Pb activity for core MUC-1B **(a)**, calcium carbonate content (%$CaCO_3$) for core MUC-1B **(b)** and core F98-1A **(c)**, magnetic susceptibility and ^{210}Pb activity for core BC-3C **(d)**, contact print of core BC-3D **(e)**, age model estimated from ^{210}Pb excess ($^{210}Pb_{xs}$) with the constant rate of supply model for core MUC-1B, including error bars representing ± one standard deviation **(f)**, and final integrated age model for core MUC-1B, including the upper 10 cm ^{210}Pb activities and stratigraphic correlation with cores BC-3 and F98-1A **(g)**. Green areas in **(a) (b), (d)**, and **(g)** correspond to the "spongy layer", whereas the cross-hatched area in the same figures represents harbor construction work starting December 2002; the shaded grey area in **(d)** represents the 1836 earthquake. The stars in **(g)** represent ages from core F98-1A obtained by correlation of %$CaCO_3$ with core MUC-1B. Ages in **(c)** and **(e)** were obtained from the original age models for core F98-1A (Vargas et al., 2007) and core BC-3D (Caniupán et al., 2009), respectively. In **(f)**, extreme non-steady state ^{210}Pb activities are enclosed within an oval.

For MUC-1B, biogenic opal, diatom valve counts, and Ba_{bio} describe similar trends (Figs. 3a–c) and, in fact, they are significantly correlated ($r > 0.5$, $p < 0.001$). In addition, chlorins and C_{org} in BC-3 show high frequency oscillations similar to those observed for other productivity proxies in cores MUC-1B and BC-3, especially before AD 1950 (Figs. 3c–e). Since the late 1950s and the early 1960s, these high frequency variations, although still present, are dampened by a strong increasing trend (Figs. 3d–e).

4.4 Paleoxygenation proxies

Depth distribution patterns of redox-sensitive element ratios Mo/Al and V/Al are similar and display high and coherent variability ($r = 0.83$, $p < 0.001$; Fig. 4). These patterns

Table 2. Diatom valve counts in selected core depths around the spongy layer for core MUC-1B collected in Mejillones Bay (northern Chile). Species are grouped by habitat and/or distribution and are expressed as relative abundance (%) (Sánchez, 2009).

Diatom habitat	Depth in core [cm] (AD years)			
	19.5–20 (1875–1871)	20.0–20.5 (1870–1867)	20.5–21 (1866–1863)	21–21.5 (1862–1858)
Oceanic/warm-temperate	14.91	18.89	43.46	18.25
Upwelling	77.05	70.46	53.95	82.80
Freshwater	0.28	0.30	0.50	0.10
Non-planktonic	0.52	0.52	0.57	0.13
Coastal planktonic	6.30	9.59	1.42	1.67
Tycoplankton	0.95	0.25	0.07	0.06
Total diatoms (valves g^{-1})	4.76×10^8	4.32×10^8	2.06×10^8	10.4×10^8

are roughly replicated by the (lycopane+n-C_{35})/n-C_{31} ratio during several periods (Figs. 4a–b). All the redox-sensitive proxies display a general trend toward higher values to the present. This trend is more pronounced for S/Al and Fe/Al proxies, which are significantly correlated with the summation of percent deviation from the mean of the terrigenous proxies Ti/Al and Zr/Al ($r > 0.25$, $p < 0.05$) (Figs. 4c, d).

5 Discussion

Cores MUC-1B and BC-3 were successfully correlated and a constrained age model was obtained for core MUC-1B in order to study the signals of oxygenation and productivity during the last two centuries in Mejillones Bay. However, because coastal upwelling areas such as the Peru-Chile margin are simultaneously characterized by high biological productivity and the formation of an oxygen minimum zone, the interpretations of proxies are not always straightforward. Consequently, we focus on the interpretation of paleoproductivity proxies as a function of bottom-water oxygenation and their related preservation.

5.1 Oxygenation and productivity proxies

Redox-sensitive trace metals in core MUC-1B are highly enriched, especially since the mid-1850s, suggesting more oxygenated conditions in the bottom water before that time. These observations are consistent with previous findings pointing to a transition period between 1820 and 1878 characterized by stronger upwelling-favorable coastal winds off northern Chile and Peru (Vargas et al., 2007; Fig. 4).

In general, the high-frequency oscillations observed in the various productivity and oxygenation proxies used herein seem closely related (Figs. 3 and 4). This is particularly true for the siliceous productivity proxies (biogenic opal and total diatom valves) in MUC-1B and for biogenic barium, which covaried with Mo/Al, V/Al, and the (lycopane+n-C_{35})/n-C_{31} ratio (Figs. 3a–c and 4a–b). It is also evident that other productivity proxies measured in core BC-3 (e.g. chlorin and C_{org}) exhibited short-term oscillations that roughly follow those of siliceous productivity (Fig. 3). However, the coherence between productivity proxies in cores MUC-1B and BC-3 is far from being perfect and, in fact, has weakened since the mid-20th century when a strong increasing trend dampened the high frequency variability of chlorins and C_{org} (Figs. 3d–e) and siliceous productivity plummeted (Figs. 3a–b). Although water column primary production in Mejillones Bay is expected to be dominated by siliceous phytoplankton (e.g. diatom) typical of coastal upwelling ecosystems, primary production based on smaller phytoplankton (i.e. pico- and nanoplankton) may be also reflected by sedimentary productivity proxies during certain periods (e.g. warming periods). In this sense, the composition of the phytoplankton community may have shifted in response to changing environment conditions such as water column stratification, nutrient supply, and the OMZ depth (Herrera and Escribano, 2006). For instance, during the 1997–1998 El Niño, the intrusion of warmer oligotrophic waters to the coast reduced upwelling in the upper 100 m off Antofagasta (northern Chile, 23° S) and "an oligotrophic regime resulted in a higher dominance of pico- and nanoplankton in inshore areas during summer/winter 1997 and summer 1998" (Iriarte and González, 2004). Therefore, whereas biogenic opal and diatom valve counts account just for siliceous productivity (i.e. microphytoplankton), other proxies such as C_{org}, chlorins, and biogenic Ba may carry a mixed signal (e.g. they respond simultaneously to the abundance of microphytoplankton, pico-, and nanoplankton), which may differ importantly from siliceous productivity proxies under oligotrophic regimes like that of El Niño (Iriarte and González, 2004).

The spongy layer in cores MUC-1B and BC was mostly deposited during the 1860s and is especially interesting because, according to most recent reconstructions, several strong El Niño (EN) and La Niña (LN) events occurred during this period (EN: 1861–1864, 1869–1871, LN: 1860–1861, 1863, 1867–1868; Table 1). Under such environmental conditions, it is not surprising to find wide fluctuations of siliceous productivity around the upper and lower boundaries of the spongy layer that are probably associated with El Niño events (i.e. decreased biogenic opal, total diatom

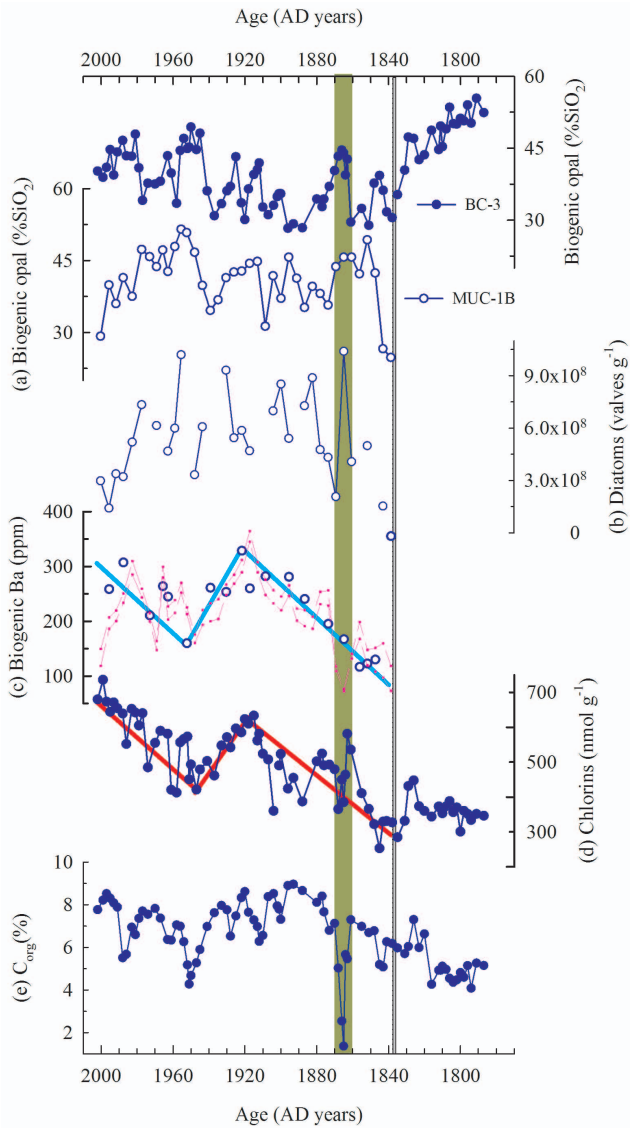

Fig. 3. Productivity proxies: biogenic opal (SiO_2) for cores MUC-1B and BC-3D **(a)**, total diatom counts (MUC-1B) **(b)**, biogenic Ba (MUC-1B): [thin pink dashed lines correspond to upper and lower limits of biogenic barium (Ba_{bio} computed from constant detrital Ba/Al of 0.001 to 0.003, corresponding to the range of direct extractions (bioBa) (open circles)] **(c)**, chlorins (BC-3D) **(d)**, and organic carbon (C_{org}, BC-3D) **(e)**. Common trends between biogenic Ba and chlorins are highlighted with blue and red lines, respectively. Green and shaded grey areas as in Fig. 2.

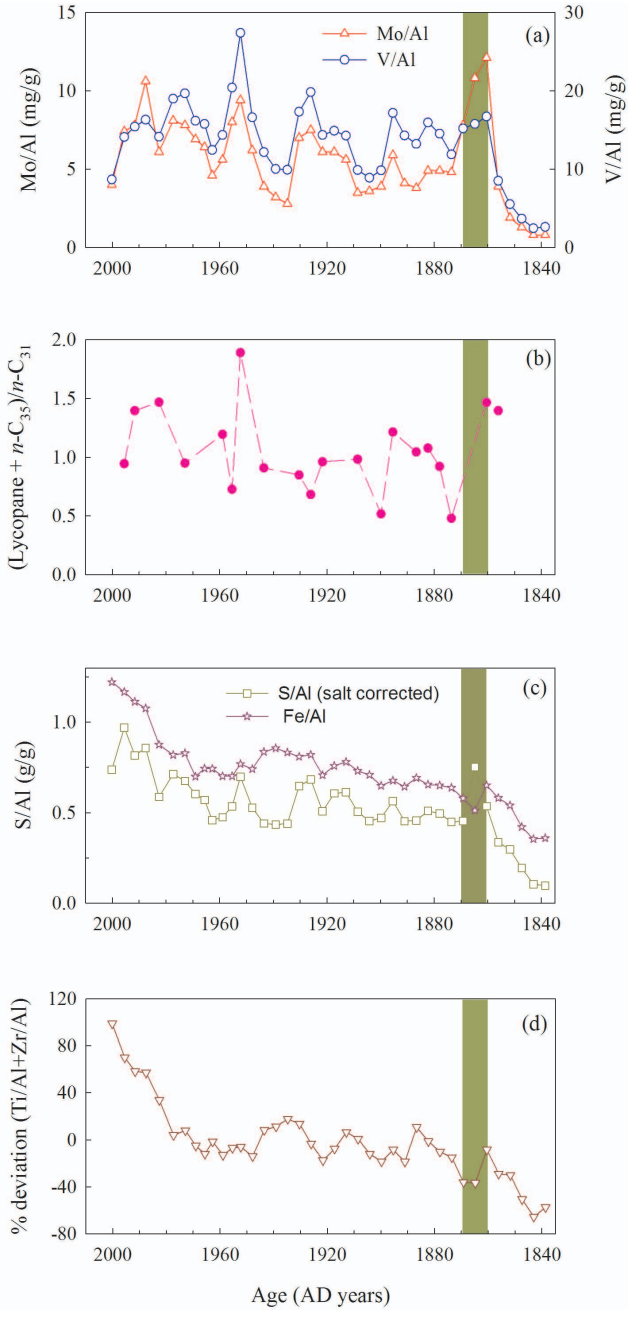

Fig. 4. Normalized bottom-water oxygenation proxies Mo/Al and V/Al **(a)**, (lycopane+n-C_{35})/n-C_{31} ratio **(b)**, S/Al (salt corrected) and Fe/Al ratios **(c)**, and summation of percent deviation from the mean of terrigenous proxies Ti/Al and Zr/Al **(d)**. All the proxies correspond to core MUC-1B. Green area as in Fig. 2.

valve counts, and chlorin). In the middle of the spongy layer, La Niña conditions (i.e. increased biogenic opal, total diatom valve counts and chlorin as well as increased sulfidic conditions) seem to dominate (Figs. 3 and 4). However, care should be taken when interpreting proxies in the spongy layer, as several other proxies tend to exhibit erratic behavior, especially in the middle of this layer (e.g. Ba_{bio} and C_{org}; Fig. 3).

Alternatively, we can use more quantitative indicators of ENSO events such as the cold tongue index (CTI; Fig. 5a) and the reconstructed/instrumental Pacific Decadal Oscillation (PDO; Fig. 5b) to better understand oxygenation responses of Mejillones Bay to large-scale ocean/climate forcing. As a result, we observe somewhat warmer sea surface

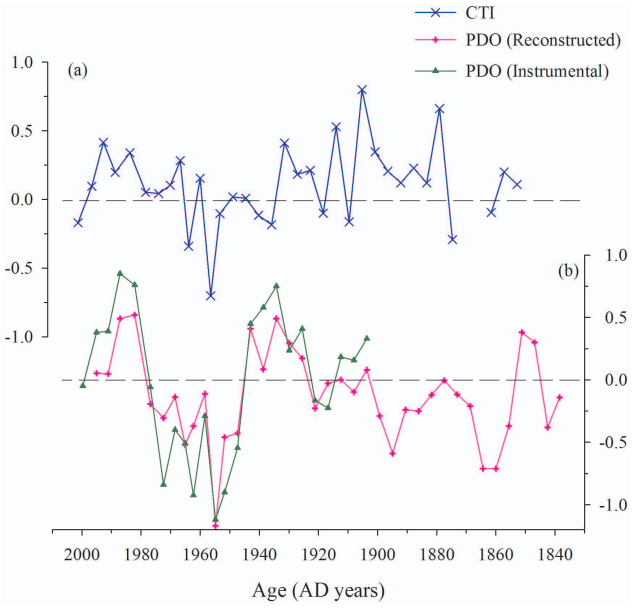

Fig. 5. The Cold Tongue Index (CTI); sea surface anomaly minus global mean in the area 6° N–6° S, 180°–90° W (http://jisao.washington.edu/enso/) **(a)** and time-series of the Pacific Decadal Oscillation (PDO) reconstructed from tree rings from North America (D'Arrigo et al., 2001) and instrumental data available from AD 1900 (Mantua et al., 1997) **(b)**. The original information was averaged to match the sampling intervals established by means of the age model estimated for core MUC-1B.

anomalies in the Equatorial Central Pacific during the second half of the 19th century as compared to the 20th century, but rather neutral or cold La Niña-like conditions in the period between the 1930s and 1960s (Fig. 5a). On the other hand, the PDO time-series revealed periods with relatively cold conditions in the northern Pacific during the 1860s, 1890s, and between the 1940s and the 1970s, whereas years such as the 1900s, 1920s–1930s, 1990s, and 2000s appeared to be dominated by warm anomalies (Fig. 5b). It should be noted that, since the 1840s, warm anomalies of the CTI have been more common than cold anomalies (Fig. 5a), resulting in substantially more overlapping between the CTI and PDO time-series during warm periods than cool periods (Fig. 5). Since both ENSO events (e.g. Iriarte and González, 2004) and the PDO (e.g. Vargas et al., 2007) have the potential to affect environment oxygenation in the study area, we propose that high frequency fluctuations in bottom-water oxygenation inferred from cores MUC-1B and BC-3 (Fig. 4) might have originated in the interaction between ENSO and PDO. This conclusion is supported, for example, by negative excursions of bottom-water oxygenation proxies (i.e. more oxygenated conditions) during the 1900s and the 1930s (Fig. 4) when positive anomalies of the CTI and PDO were in phase (Fig. 5). On the other hand, positive excursions of redox proxies tend to coincide with periods of negative PDO anomalies (e.g. 1855–1865, 1890s, 1945–1955, and 1960–1975; Figs. 4, 5). Because of the correlation between productivity and bottom-water oxygenation, the patterns associated with the ENSO and the PDO must also be linked to productivity changes.

5.1.1 Sulfidic conditions and preservation issues

The close relationship between S/Al and Fe/Al (Fig. 4c) suggests that a significant portion of reduced sulfur in the sediment is incorporated into metallic sulfides such as pyrite (Böning et al., 2005). It is also supported by the general pattern of biogenic Ba that corresponds to those for chlorins and C_{org} and correlates with S/Al (Figs. 3c–d and 4). Therefore, we suggest that between ∼AD 1840 and ∼AD 1870, bottom water and sediments in Mejillones Bay experienced a transition to stronger sulfidic conditions. Such conditions remained more or less stable with a pattern of increasing variability between ∼1870 and the late 1960s. Eventually, this pattern ended during the early 1970s when a new and rapid excursion toward maximal S/Al ratios occurred in coincidence with an inflexion to higher terrigenous input (Figs. 4c–d).

In addition, it has been suggested that organic carbon preservation depends on the redox conditions in surface sediments (e.g. Sun et al., 2002) and successive oxygenation oscillations would have the net effect of reducing preservation of chlorophyll and degradation products (Sun et al., 1993). In this sense, the increased frequency of ENSO events documented since the second half of the 20th century (e.g. Trenberth, 1997) might have produced a combined productivity-preservation signal in the sedimentary record of Mejillones Bay due to fluctuations in the oxygenation of bottom waters and surface sediments. It is interesting to note that S/Al and chlorins showed an increasing trend towards the present (i.e. since the 1960s). No such trend is clearly observed in C_{org}, suggesting increased preservation of chlorins under stronger sulfidic conditions supported by the evidence of less efficient degradation of chlorophyll in anoxic than oxic sediments (Sun et al., 1993). Based on the latter interpretation, the productivity and bottom-water oxygenation proxies analyzed in this work provide evidence to confirm the hypothesis proposed by Vargas et al. (2007) that the marine coastal ecosystem off northern Chile has experienced a shift since the mid 19th-century towards increased biological productivity due to stronger upwelling-favorable winds. This is consistent with the observed increase of proxies of terrigenous input Ti/Al, Zr/Al, Fe/Al, and magnetic susceptibility (Fig. 4d). However, the most recent increments of export productivity in the study area suggested by the increase in the content of sedimentary biogenic Ba and chlorins (Figs. 3c–d) do not seem to be related to siliceous export productivity (actually, siliceous productivity has been decreasing during the last ∼40 years; Figs. 3a–b), indicating a change in the phytoplankton community composition coincident with the strongest sulfidic conditions experienced

in Mejillones Bay during the last ∼150 years. In summary, increased sulfidic conditions observed during the last few decades in Mejillones Bay do not appear to be particularly associated with high export production but rather with oxygen-poor water-mass advection due to increased upwelling off Angamos Point (e.g. Vargas et al., 2007).

6 Conclusions

During the last two centuries, the sediment of Mejillones Bay has recorded what seems to be a shift from relatively higher oxygenation conditions to a less oxygenated state in the coastal marine ecosystem off northern Chile, characterized by intense ENSO-like activity and large fluctuations of both biological export productivity and bottom water oxygenation. In the long term, such variability has resulted in more reducing conditions in bottom water and sediments that appear to have intensified since the early 1960s and were probably accompanied by shifts in the composition of the phytoplankton community. These findings provide insights as to the response of the upwelling ecosystem of northern Chile to recent climate change.

Acknowledgements. This research was funded by FONDECYT grant 3090040 (JADO), FONDECYT grant 1040503 (SP), and the Center for Oceanographic Research in the eastern South Pacific (COPAS), University of Concepción. We acknowledge the valuable help of A. Avila, L. Nuñez, and R. Castro for laboratory assistance, and the Associate Editor A. Boetius, A. Reitz and one anonymous reviewer. JADO acknowledges the support of POGO and the agreement Fundación Andes/Woods Hole Oceanographic Institution/University of Concepción for funding two research visits to the Marine Geochemistry Laboratory, at Utrecht University.

Edited by: A. Boetius

References

Appleby, P. G. and Oldfield, F.: The calculation of lead-210 dates assuming a constant rate of supply of unsupported 210Pb to the sediment, Catena, 5, 1–8, 1978.

Arntz, W. E., Gallardo, V. A., Gutiérrez, D., Isla, E., Levin, L. A., Mendo, J., Neira, C., Rowe, G. T., Tarazona, J., and Wolff, M.: El Niño and similar perturbation effects on the benthos of the Humboldt, California, and Benguela Current upwelling ecosystems, Adv. Geosci., 6, 243–265, doi:10.5194/adgeo-6-243-2006, 2006.

Binford, M.: Calculation and uncertainty analysis of 210Pb dates for PIRLA project lake sediment cores, J. Paleolimnol., 3, 253–267, 1990.

Blanco, J., Carr, M.-E., Thomas, A., and Strub, T.: Hydrographic conditions off northern Chile during the 1996-1997 La Niña and El Niño events, J. Geophys. Res., 107(C3), doi:10.1029/2001JC001002, 2002.

Böning, P., Cuypers, S., Grunwald, M., Schnetger, B., and Brumsack, H-J.: Geochemical characteristics of Chilean upwelling sediments at ∼36°S, Mar. Geol., 220, 1–21, 2005.

Caniupán, M., Villaseñor, T., Pantoja, S., Lange C. B., Vargas, G., Muñoz, P., and Salamanca, M.: Sedimentos laminados de la Bahía Mejillones como registro de cambios temporales en la productividad fitoplanctónica de los últimos ∼200 años, Revista Chilena de Historia Natural, 82, 83–96, 2009.

Chan, F., Barth, J., Lubchenco, J., Kirincich, A., Weeks, H., Peterson, W., and Menge, B.; Emergence of anoxia in the California Current Large Marine Ecosystem, Science, 319, 920, doi: 10.1126/science.1149016, 2008.

Chavez, F., Bertrand, A., Guevara-Carrasco, R., Soler, P., and Csirke, J.: The northern Humboldt Current System: Brief history, present status and a view towards the future, Prog. Oceanogr., 79, 95–105, 2008.

D'Arrigo, R., Villalva, R., and Wiles, G.: Tree-ring estimates of Pacific decadal climate variability, Clim. Dynam., 18, 219–224, 2001.

Diaz, R. and Rosenberg, R.: Spreading dead zones and consequences for marine ecosystems, Science, 231, 926–929, 2008.

Díaz-Ochoa, J. A., Lange, C. B., and De Lange, G. J.: Preservación y abundancia de escamas de peces en sedimentos del margen continental de Chile (21–36° S), Revista Chilena de Historia Natural, 81, 561–574, 2008.

Escribano, R.: Population dynamics of *Calanus chilensis* in Chilean eastern boundary Humboldt Current, Fish. Oceanogr., 7, 245–251, 1998.

Fréon, P., Barange, M., and Aristegui, J.: Eastern Boundary Upwelling Ecosystems: Integrative and comparative approaches, Prog. Oceanogr., 83, 1–14, 2009.

Fuenzalida, R., Schneider, W., Garcés-Vargas, J., Bravo, L., and Lange, C.: Vertical and horizontal extension of the oxygen minimum zone in the eastern South Pacific Ocean, Deep Sea Res. Pt. II, 56, 992–1003, 2009.

Garcia-Herrera, R., Diaz, H. F., Garcia, R. R., Prieto, M. R., Barriopedro, D., Moyano, R., and Hernandez, E.: A chronology of El Niño events from primary documentary sources in northern Peru, J. Climate, 21, 1948–1962, doi:10.1175/2007JCLI1830.1, 2008.

Gergis, J. and Fowler, A.: A history of ENSO events since A.D. 1525: implications for future climate change, Climatic Change, 92, 343–387, 2009.

González, H., Daneri, G., Figueroa, D., Iriarte, J., Lefevre, N., Pizarro, G., Quiñones, R., Sobrazo, M., and Troncoso, A.: Producción primaria y su destino en la trama trófica pelágica y océano profundo e intercambio océano-atmósfera de CO_2 en la zona norte de la corriente de Humboldt (23° S): posibles efectos del evento El Niño, 199798 en Chile, Revista Chilena de Historia Natural, 71, 42–458, 1998.

Grillet, L., Ratliff, M., Montgomery, R., and Monter, E.: Chile Mejillones Port Project (CH-0162): Environmental and social impact report (ESIR), Inter-American Development Bank, 50 p, http://www.iadb.org/pri/projDocs/CH0162_R_E.pdf, last access: December 2009, 2001.

Helly, J. and Levin, L.: Global distribution of naturally occurring marine hypoxia on continental margins, Deep-Sea Res. Pt. I, 51, 1159–1168, 2004.

Herrera, L. and Escribano, R.: Factors structuring the phytoplankton community in the upwelling site off El Loa River in northern Chile, J. Mar. Syst., 61, 13–38, 2006.

Iriarte, J., Pizarro, G., Troncoso, V., and Sobarzo, M.: Primary pro-

duction and biomass size-fractioned phytoplankton off Antofagasta, Chile (23–24° S) during pre-El Niño and El Niño 1997, J. Mar. Syst., 26, 37–51, 2000.

Iriarte, J. and González, H.: Phytoplankton size structure during and after the 1997/98 El Niño in a coastal upwelling area of the northern Humboldt Current System, Mar. Ecol. Prog.-Ser., 269, 83–90, 2004.

Keeling, R., Körtzinger, A., and Gruber, N.: Ocean deoxygenation in a warming world, Annu. Rev. Mar. Sci., 2, 199–229, 2010.

Kimble, B., Maxwell, J., Philp, R., Eglinton, G., Albrecht, P., Ensminger, A., Arpino, P., and Ourisson, G.: Tri- and tetraterpenoid hydrocarbons in the Messel oil shale, Geochim. Cosmochim. Ac., 38, 1165–1181, 1974.

Mantua, N., Hare, S., Zhang, Y., Wallace, J, and Francis, R.: A Pacific interdecadal oscillation with impacts on salmon production, B. Am. Meteorol. Soc., 78, 1069–1079, 1997.

Marín, V., Rodríguez, L., Vallejo, L., Fuenteseca, J., and Oyarce, E.: Dinámica primaveral de la productividad primaria de Bahía Mejillones del Sur (Antofagasta, Chile), Revista Chilena de Historia Natural, 66, 479–491, 1993.

Marín, V., Escribano, R., Delgado, L. E., Olivares, G., and Hidalgo, P.: Nearshore circulation in a coastal upwelling site off the northern Humboldt Current System, Cont. Shelf Res., 21, 1317–1329, 2001.

Marín, V., Delgado, L., and Escribano, R.: Upwelling shadows at Mejillones Bay (northern Chilean coast): remote sensing in situ analysis, Investigaciones Marinas, Valparaíso, 31, 47–55, 2003.

Monteiro, P., Plas, A., Mélice, J.-L., and Florenchie, P.: Interannual hypoxia variability in a coastal upwelling system: Ocean-shelf exchange, climate ecosystem-state implications, Deep-Sea Res. Pt. I, 55, 436–450, 2008.

Mortlock, R. and Froelich, P.: A simple method for rapid determination of biogenic opal in pelagic marine sediments, Deep-Sea Res., 36, 1415–1426, 1989.

Nameroff, T., Calvert, S., and Murray, J: Glacial-interglacial variability in the Eastern Tropical North Pacific oxygen minimum zone recorded by redox-sensitive trace metals, Paleoceanography, 19, PA1010, doi:10.1029/2003PA000912, 2004.

Ortlieb, L., Escribano, R., Follegati, R., Zúñiga, O., Kong, I., Rodríguez, L., Valdés, J., Guzman, N., and Iratchet, P.: Recording of ocean-climate changes during the last 2,000 years in a hypoxic marine environment off northern Chile (23° S), Revista Chilena de Historia Natural, 73, 221–242, 2000.

Quinn, W., Neal, V., and Antunez, S.: El Niño occurrence over the past four and half centuries, J. Geophys. Res., 92(C13), 14449–14461, 1987.

Quinn, W.: The large-scale ENSO event, the El Niño, and other important features, Bulletin de l'Institut Français d'Études Andines, 22(1), 13–34, 1993.

Reitz, A., Pfeifer, K., De Lange, G. J., and Klump, J.: Biogenic barium and the detritial Ba/Al ratio: a comparison of their direct and indirect determination, Mar. Geol., 204, 289–300, 2004.

Rutten, A. and De Lange, G. J.: A novel selective extraction of barite, and its application to eastern Mediterranean sediments, Earth Planet. Sci. Lett., 198, 11–24, 2002.

Sánchez, G. E.: Variabilidad de la producción silícea durante los últimos doscientos años, basada en diatomeas planctónicas y sílice biogénico en sedimentos del margen continental de Chile, Ph.D Thesis, Universidad de Concepción, Concepción (Chile), 211 p., 2009.

Schenau, S. and De Lange, G. J.: A novel chemical method to quantify fish debris in marine sediments, Limnol. Oceanogr., 45, 963–971, 2000.

Siffedine, A., Gutiérrez, D., Ortlieb, L., Boucher, H., Velazco, F., Field, D., Vargas, G., Boussafir, M., Salvatecci, R., Ferreira, V., García, M., Valdés, J., Caquineau, S., Mandeng Yogo, M., Cetin, F., Solis, J., Soler, P., and Baumgartner, T.: laminated sediments from the Peruvian continental slope: A 500 year record of upwelling system productivity, terrestrial runoff and redox conditions, Prog. Oceanogr., 79, 190–197, 2008.

Sinninghe Damsté, J., Kuypers, M., Schouten, S., Schulte, S., and Rullkötter, J.: The lycopane/C31 n-alkane ratio as a proxy to assess palaeoxicity during sediment deposition, Earth Planet. Sci. Lett., 209, 215–226, 2003.

Stramma, L., Jhonson, G., Sprintall, J., and Mohrholz, V.: Expanding oxygen-minimum zones in the tropical oceans, Science, 320, 655–658, 2008.

Strub, P. T., Mesías, J. M., Montecino, V., Rutllant, J., and Salinas, S.: Coastal ocean circulation off western South America, in: Coastal segment (6,E), edited by: Robinson, A. R. and Brink, K. H., The Sea, 11, 273–308, 1998.

Sun M., Lee, C., and Aller, R.: Laboratory studies of oxic and anoxic degradation of chlorophyll-a in Long Island Sound sediment, Geochim. Cosmochim. Ac., 57, 147–157, 1993.

Sun, M., Aller, R., Lee, C., and Wakeham, S.: Effects of oxygen and redox oscillation on degradation of cell-associated lipids in superficial marine sediments, Geochim. Cosmochim. Ac., 66, 2003–2012, 2002.

Trenberth, K. E: The definition of El Niño, Bull. Am. Meteorol. Soc., 78, 2771–2777, 1997.

Valdés, J., Ortlieb, L., and Sifeddine, A.: Variaciones del sistema de surgencia de Punta Angamos (23° S) y la zona de mínimo oxígeno durante el pasado reciente. Una aproximación desde el registro sedimentario de la Bahía Mejillones del Sur, Revista Chilena de Historia Natural, 76, 347–362, 2003.

Valdés, J., Sifeddine, A., Lallier-Verges, E, and Ortlieb, L.: Petrographic and geochemical study of organic matter in surficial laminated sediments from an upwelling system (Mejillones del Sur Bay, northern Chile), Org. Geochem., 35, 881–894, 2004.

Vargas, G., Ortlieb, L., Pichon, J. J., Bertaux, J., and Pujos, M.: Sedimentary facies and high resolution primary production inferences from laminated diatomaceous sediments off northern Chile (23° S), Mar. Geol., 211, 79–99, 2004.

Vargas, G., Pantoja, S., Rutllant, J., Lange, C.B., and Ortlieb, L.: Enhancement of coastal upwelling and interdecadal ENSO-like variability in the Peru-Chile Current since the late 19^{th} century, Geophys. Res. Lett., 34, L13607, doi:10.1029/2006GL028812, 2007.

Volkman, J.: Lipid Markers for Marine Organic Matter, The Handbook of Environmental Chemistry, 2, 27–70, 2005.

Zheng, Y., Anderson, R., Geen, A. van, and Kuwabara, J.: Authigenic molybdenum formation in marine sediments: A link to pore water sulfide in the Santa Barbara basin, Geochim. Cosmochim. Ac., 64, 4165–4178, 2000.